

# A *Fusarium Oxysporum*-derived Compound Exhibits Potential Insecticidal Activity against Cotton Bollworm: Evidence from *In Silico* and *In Vitro* Analyses



Saeed Ullah Khattak<sup>1,\*</sup>, Muhammad Salim<sup>1</sup>, Sajjad Ahmad<sup>2,3,\*</sup>, Norah Abdullah Albekairi<sup>4</sup>, Abdulrahman Mohammed Alshammari<sup>4</sup> and Dong-Qing Wei<sup>3</sup>

<sup>1</sup>Center of Biotechnology and Microbiology, University of Peshawar, Peshawar 25000, Pakistan

<sup>2</sup>Department of Health and Biological Sciences, Abasyn University, Peshawar 25000, Pakistan

<sup>3</sup>Zhongjing Research and Industrialization Institute of Chinese Medicine, Zhongguancun Scientific Park, Nayang, P.R. China

<sup>4</sup>Department of Pharmacology and Toxicology, College of Pharmacy, King Saud University, Riyadh, 11451, Saudi Arabia

## Abstract:

**Introduction:** Fungal derived secondary metabolites serve as promising alternatives to traditional insecticides due to their eco-friendly nature and specific modes of action. This study investigates the insecticidal potential of a secondary metabolite derived from *Fusarium oxysporum* using *in silico* and *in vitro* approaches. The objectives include the purification of the bioactive compound, followed by computational and experimental evaluations to assess its insecticidal efficacy.

**Methods:** The initial purification involved mass spectroscopic analysis, followed by structural elucidation using Varian 500 NMR. The compound was tested for insecticidal potential using third instar nymphs of *Helicoverpa armigera*. From stock solution prepared in sterile dimethyl sulfoxide (DMSO) test concentrations of 100, 250, 500, and 1000 µg mL<sup>-1</sup> were prepared. Imidacloprid in powder form was used as the standard insecticide in this experiment, also at concentrations of 100, 250, 500, and 1000 µg mL<sup>-1</sup>. Computational analyses, including molecular docking, molecular dynamics simulations and binding free energy calculations, were performed to explore the compound's interaction with the target receptor.

**Results:** The compound derived from *F. oxysporum* was identified as 6-butyl-3-(1-hydroxyethyl)-2-methyl-2H-pyran-5-carbonyl carbamic acid having an exact mass of 283 and molecular formula C<sub>14</sub>H<sub>21</sub>NO<sub>5</sub>. The fungal compound, administered at concentrations of 100, 200, and 250 µg mL<sup>-1</sup>, exhibited mortality rates of 30%, 56.6%, and 63.3%, respectively. In comparison, the standard drug, imidacloprid, demonstrated mortality rates of 30%, 50%, and 60% at the respective concentrations. At a concentration of 500 µg mL<sup>-1</sup>, the fungal compound inhibited the growth of 8 larvae in each test plate, resulting in an 80% mortality rate while, the standard at this concentration caused the death of 8 larvae in two petriplates and 7 larvae in the third, resulting in a mortality rate of 76.6%. At the highest applied concentration (1000 µg mL<sup>-1</sup>), both the fungal compound and the standard exhibited 100% mortality by inhibiting the growth of every larva in all petriplates. The docking analysis predicted -5.3 binding energy that represents the selected compound having significant binding affinity for the target receptor. Similarly, the compound showed stable dynamics with the enzyme and reported robust binding energies.

**Discussion:** The findings highlight the potential of 6-butyl-3-(1-hydroxyethyl)-2-methyl-2H-pyran-5-carbonyl carbamic acid as a bioactive fungal metabolite for eco-friendly pest control, warranting further investigations into its mechanism of action, field efficacy, and environmental safety. Future work will focus on chemical synthesis to produce the compound in sufficient quantities for comprehensive biological evaluations, including detailed toxicity profiling, selectivity assessments and environmental safety studies. Additionally, field trials will be conducted to evaluate its real-world efficacy in pest management.

**Conclusion:** This study demonstrates that 6-butyl-3-(1-hydroxyethyl)-2-methyl-2H-pyran-5-carbonyl carbamic acid exhibits potent insecticidal activity against *Helicoverpa armigera*, with efficacy comparable to imidacloprid.

**Keywords:** *Helicoverpa armigera*, Fungal secondary metabolite, Bio-insecticide, Imidacloprid, NMR, LCMS.

© 2025 The Author(s). Published by Bentham Open.

This is an open access article distributed under the terms of the Creative Commons Attribution 4.0 International Public License (CC-BY 4.0), a copy of which is available at: <https://creativecommons.org/licenses/by/4.0/legalcode>. This license permits unrestricted use, distribution, and reproduction in any medium, provided the original author and source are credited.



Received: December 27, 2024

Revised: March 12, 2025

Accepted: April 11, 2025

Published: June 11, 2025



Send Orders for Reprints to  
[reprints@benthamscience.net](mailto:reprints@benthamscience.net)

\*Address correspondence to these authors at the Center of Biotechnology and Microbiology, University of Peshawar, Peshawar 25000, Pakistan, Department of Health and Biological Sciences, Abasyn University, Peshawar 25000, Pakistan and Zhongjing Research and Industrialization Institute of Chinese Medicine, Zhongguancun Scientific Park, Nayang, P.R. China; E-mails: [Khattak@uop.edu.pk](mailto:Khattak@uop.edu.pk), [sahmad@bs.qau.edu.pk](mailto:sahmad@bs.qau.edu.pk) and [sajjad.ahmad@abasyn.edu.pk](mailto:sajjad.ahmad@abasyn.edu.pk)

Cite as: Khattak S, Salim M, Ahmad S, Albekairi N, Alshammari A, Wei D. A *Fusarium Oxysporum*-derived Compound Exhibits Potential Insecticidal Activity against Cotton Bollworm: Evidence from *In Silico* and *In Vitro* Analyses. *Open Biotechnol J*, 2025; 19: e18740707381303. <http://dx.doi.org/10.2174/0118740707381303250527070137>

## 1. INTRODUCTION

Insect pest management remains a significant challenge in global agriculture, leading to widespread reliance on synthetic chemical pesticides [1, 2]. However, growing concerns regarding their environmental impact and risks to human health have prompted the search for safer and more sustainable alternatives [3]. The harmful effects of synthetic pesticides, extensively documented in the United Nations Environmental Program's 1997 report, include threats to human and animal health and large-scale environmental contamination [4]. These concerns highlight the urgent need for eco-friendly pest control strategies that minimize chemical residues and reduce ecological imbalances [5, 6]. Fungal-derived metabolites have emerged as promising alternatives for insect control due to their biodegradability, target specificity, and reduced environmental toxicity [7]. These metabolites, produced as part of fungal secondary metabolism, exhibit precise modes of action with minimal collateral damage to non-target organisms [8]. Their ecological benefits, including potential synergistic interactions with other biological control agents, make them as valuable tools for sustainable pest management [9, 10].

The transition toward fungal-based insecticides requires a deeper understanding of their biochemical mechanisms and ecological effects. Advances in biotechnology and fermentation techniques have facilitated large-scale production and extraction of fungal metabolites, significantly enhancing their accessibility for agricultural applications [11]. Several fungal species, including *Beauveria bassiana*, *Metarhizium anisopliae*, and *Paecilomyces* spp., have demonstrated strong insecticidal properties against a diverse range of pests [12-14].

The integration of modern computational tools has revolutionized our understanding and application of fungal secondary metabolites [15, 16]. Techniques such as molecular modeling, simulation, and pharmacophore modeling enable researchers to predict the biological activities, molecular targets, and structural properties of fungal metabolites with exceptional precision [17, 18]. This multidisciplinary approach not only broadens our knowledge base but also paves the way for innovative and sustainable pest management strategies. Recent studies have highlighted the potential of fungal metabolites to not only act as potent insecticides but also contribute to the development of resistance management strategies by targeting specific biochemical pathways in pests [19]. Moreover, the ecological benefits of using fungal-derived insecticides are significant, as they often ex-

hibit specificity towards target pests while being less harmful to non-target organisms and the environment. This aligns with the growing demand for sustainable agricultural practices that are environmentally friendly and reduce harm to nature [20]. The continuous exploration and characterization of fungal secondary metabolites, supported by advancements in computational biology and biotechnology, are essential for the next generation of eco-friendly and effective insecticides [21].

In the current study, we report the purification and characterization of a secondary metabolite derived from *F. oxysporum* with potential insecticidal properties. After purification and structural elucidation, the compound was subjected to molecular docking and simulation studies to predict its biological activity and molecular targets. Based on the *in silico* findings, the insecticidal potential of the compound was further evaluated through *in vitro* bioassays against *Helicoverpa armigera*.

## 2. METHODOLOGY

The flow diagram of the applied methodology is shown in Fig. (1).

### 2.1. Rhizosphere Sample Processing and Isolation of Fungal Strains

Samples were obtained from the soil surrounding the roots of ginger plants (*Zingiber officinale*) cultivated in the botanical garden of the Department of Botany, University of Peshawar. Fungal isolation was achieved through the soil dilution plate method, followed by inoculation of the samples onto Potato Dextrose Agar (PDA) for ten (10) days at 28°C [22]. Upon completion of the incubation period and visual inspection of fungal growth, the fungal strains were subsequently sub-cultured and purified.

### 2.2. Identification of the Bioactive Fungal Strain

The bioactive fungal strain was identified through a series of bioactivity tests, leading to its selection for further analysis and purification of secondary metabolites. Identification of fungal strains involved analyzing various traits, including hyphal structure, colony morphology, and the arrangement of conidia. Colony pigmentation was evaluated by cultivating the strains on different media, such as Potato Dextrose Agar (PDA), Czapek Dox Agar (CDA), and Sabouraud Dextrose Agar (SDA). Hyphal morphology, spore structure, and arrangement were examined using a light microscope and the slide culture technique. To enhance visualization, slides were stained with lactophenol blue [23-25].

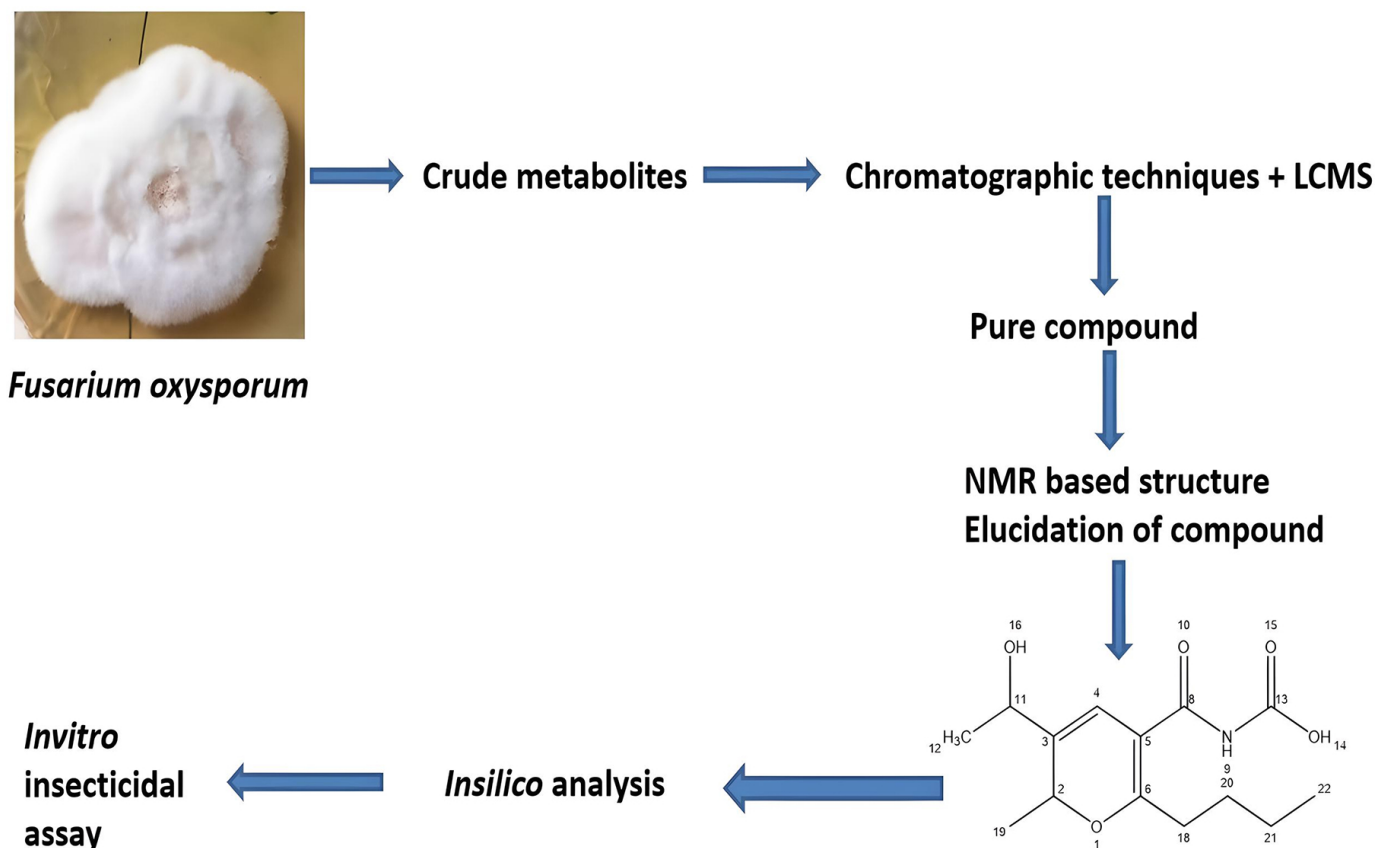


**Fig. (1).** Schematic flow of the current study.

### 2.3. Fungal Metabolites Production and Extraction using Yeast Extract Supplemented (YES) Medium

For the production of crude metabolites, a fungal culture was cultivated in a modified yeast extract-supplemented (YES) medium. To formulate a liter of YES medium optimized for fungal metabolite production, yeast extract, peptone, and glucose were dissolved in distilled water at concentrations of 2% (w/v) each. Additionally, sucrose (2% w/v) was added to serve as an alternative carbon source, while ammonium sulfate (0.5% w/v) was introduced to augment nitrogen availability. Ensuring robust growth and metabolic activity, a trace element solution including iron sulfate (0.01% w/v), zinc sulfate (0.001% w/v), copper sulfate (0.0001% w/v), and manganese sulfate (0.0001% w/v) was incorporated. The pH of the medium was precisely adjusted to 5.8 before autoclaving at 121°C [26, 27]. Sterility confirmation was conducted through overnight incubation at 28°C. After inoculation with the desired fungal strain, the medium was transferred to a shaking incubator and maintained at 28°C and 150 rpm for 14 days.

To expedite the separation and sedimentation of media components, approximately 300 µL of 35% hydrochloric acid (HCl) was added to each flask. The mycelia were homogenized using an electric blender, after which an equal volume of ethyl acetate was introduced to each flask. The mixture was intermittently mixed and shaken for 30 minutes. The mycelia were then filtered using chee-

secloth. The organic layer was separated from the resulting mixture using a separating funnel and washed with a 2M brine solution to remove impurities. Anhydrous sodium sulfate ( $\text{Na}_2\text{SO}_4$ ) was employed to dehydrate the organic layer and remove any residual moisture [28, 29]. The organic layer, containing the metabolites in crude form, was filtered again with the help of filter paper and transferred to a rotary evaporator set at 45°C to concentrate the metabolites. The dried crude extract was collected from the rotary evaporator flask by rinsing it with methanol.

### 2.4. Purification and Analysis of Fungal Metabolites

For the purification and analysis of the fungal metabolites, a combination of equipment was employed. This included the Waters 2795HT HPLC system, linked with a Waters 2998 photodiode array detector and a Micro-Mass ZQ spectrometer, enabling liquid chromatography-mass spectrometry (LCMS) analysis. The UV detection range of the instrument spanned from 200 to 400 nm. The solvent system utilized for both analytical and preparative runs comprised HPLC-grade ultrapure water, HPLC-grade methanol (MeOH), and HPLC-grade acetonitrile ( $\text{CH}_3\text{CN}$ ), supplemented with a minimal quantity of formic acid (0.055 %). Initially, a 20 µL injection was administered for the analytical run, with subsequent increases in volume for further purification processes.

## 2.5. NMR-based Structural Elucidation of the Fungal Pure Compound

One-dimensional and two-dimensional NMR spectra ( $^1\text{H}$ ,  $^{13}\text{C}$ , and HSQC) were acquired utilizing a 500 MHz Varian NMR machine. Chemical shifts, denoted in ppm, were calibrated using tetramethylsilane (TMS) as the internal standard. For examination, a solution comprising 5 mg of the pure compound dissolved in 0.65 mL of deuterated chloroform was prepared, and a series of one-dimensional and two-dimensional NMR experiments were carried out on a 500 MHz NMR spectrometer.

## 2.6. Molecular Docking Investigation

The molecular docking technique was then used to investigate the binding conformation and affinity of the compound for any given insecticidal macromolecule [30]. In this study, Glutathione S-transferase (PDB ID: 1R5A) from *Anopheles cracens* was used as a receptor [31]. The compound structure was drawn using ChemDraw 12.0 (Milne, G.W., 2010) and subsequently energy-minimized using UCSF Chimera 1.17 [32]. The enzyme receptor was also energy minimized using the steepest descent and conjugate gradient algorithms over a total of 3000 rounds. Both the compound and the enzyme receptor were saved as pdb files. Docking analysis was accomplished using PyRx 0.8 software [33]. The grid box around the enzyme active site was set considering dimensions of 30 Å along XYZ. For the compound, 100 poses were generated, and the top binding mode was selected based on negative binding energy. The complex was visualized using Discovery Studio v2021 [34].

## 2.7. Molecular Dynamics Simulation and Binding Free Energies Analysis

The dynamic movements of the docked complex were studied using molecular dynamics simulation through AMBER v22 software [35]. The complex initial processing was done using an antechamber program. The enzyme was treated using the FF19SB force field, while the compound was processed with GAFF2 [36, 37]. The simulation protocol was achieved using four phases: energy minimization, heating, equilibrium, and production run [38]. The temperature control during the production run was done using the Langevin algorithm, while the SHAKE was employed to constrain hydrogen bonds [39]. The CPPTRAJ module was used for plotting different simulation-based graphs [40]. The binding free energies were calculated using the MMPBSA.py module for over 10,000 frames from simulation trajectories [41].

### 2.7.1. In vitro Insecticidal Potential of the Pure Compound

Third-instar nymphs of *H. armigera* were obtained from the entomology department at the University of Agriculture Peshawar and placed in sterile jars containing synthetic medium. The larvae were reared in a controlled laboratory environment at 30°C and 75% relative humidity and fed a synthetic diet primarily composed of chickpea flour. The diet consisted of specific quantities of various components: 50 g of chickpea flour, 5 g of wheat germ, 12 g of yeast extract, 3.5 g of casein, 0.5 g of sorbic acid, and 1 g of met-

hylparaben in 150 mL of distilled water for the mixture (A); 0.35 g of choline chloride, 0.02 g of streptomycin sulfate, 2 g of ascorbic acid, 0.15 g of cholesterol, a multivitamin multi-mineral capsule (manufactured by GlaxoSmithKline Pharmaceuticals Limited), 200 mg of vitamin E, 1 mL of formaldehyde, 0.3 g of bavistin, and 30 mL of distilled water for the mixture (B); and 6.5 g of agar in 180 mL of distilled water for mixture (C). Components A and B were combined and then mixed with molten agar (C). This medium was also used to conduct insecticidal activity by pouring 22 mL of the medium into each petriplate.

A stock solution of the pure compound was prepared at a concentration of 5 mg mL<sup>-1</sup> in sterile dimethyl sulfoxide (DMSO). Test samples were prepared from this stock solution with dose concentrations of 100, 250, 500, and 1000 µg mL<sup>-1</sup> by adding them to the non-solidified medium in the Petri plates. Each was marked with the respective concentration at the time when molten agar was added. Imidacloprid (Rudolf Pakistan) in powder form was used as the standard insecticide in this experiment, also at concentrations of 100, 250, 500, and 1000 µg mL<sup>-1</sup>. Ten larvae of *H. armigera* were placed in each Petri plate marked with the respective concentration of the fungal compound and the standard insecticide. A control treatment was maintained, consisting of only the medium and larvae. Each treatment was performed in triplicate under laboratory conditions at 30°C and 75% relative humidity.

## 3. RESULTS

### 3.1. Identification of Fungal Strains

On PDA medium, the colony color was initially white, then becoming more pinkish with the growth of the fungus over time. The colony was observed to be Fast-growing, spreading colonies that were initially circular but later became slightly irregular with age. On PDA medium, the colonies were dense but fluffy and cottony in appearance. In comparison, the same colonies on SDA and Czapek dox agar medium appeared less vibrant, more compact, and slow-growing. On the PDA medium, the colony surface was more wrinkled, specifically at the center, but on SDA and CDA medium the colony surface was smoother and even in comparison to the PDA medium (Fig. 2A). Microscopic identification was performed by observing conidia and conidiophores by staining it with lactophenol cotton blue stain and observing at 2000x using a compound microscope. The conidia were observed as small unicellular and microscopic with a dark grayish shade inside the conidiophore. The fungus under study was identified through its slenderical, erect but slightly curved shaped conidiophores which were observed both solitary and in clusters under the compound microscope (Fig. 2B).

### 3.2. Purification and Mass Determination of the Pure Compound

The crude extract obtained was subjected to purification via flash column chromatography, employing ethyl acetate and n-hexane as solvent systems. The elution of the pure compound was achieved utilizing a solvent system with a polarity of 85%. Subsequently, the comp-



ound underwent analysis by LCMS, employing an analytical setup comprising a Phenomenex Luna C-18 column, a PDA detector sensitive to secondary metabolites within the UV range of 200-400 nm, an autosampler, and an auto fraction collector. Following the analytical run, the pure compound exhibited a mass of 283 (Fig. 3A). For the preparative run, a total of 41.8 mg of crude extract was utilized. A concentration of 40 mg mL<sup>-1</sup> of the crude extract in HPLC-grade methanol was prepared for the preparative run, resulting in the purification of 7.24 mg of the pure compound. The preparative process entailed a series

of 37 runs each lasting for 30 minutes. The LCMS chromatogram unveiled a UV profile with a maximum wavelength ( $\lambda_{\text{max}}$ ) at 281 nm. The compound exhibited an electrospray (ES) profile at 282 and an electrospray (ES<sup>+</sup>) profile at 284 [M]<sup>+</sup>H and 306 [M]<sup>+</sup>Na<sup>+</sup>, aligning with the molecular formula C<sub>14</sub>H<sub>21</sub>NO<sub>5</sub> [calculated as C<sub>14</sub>H<sub>21</sub>NO<sub>5</sub> + Na = 306.14] (Fig. 3B). The retention time for the compound was established at 9.6 minutes. The analysis confirmed the molecular formula of C<sub>14</sub>H<sub>21</sub>NO<sub>5</sub> and an exact mass of 283.14 for the compound under study (Fig. 3C).

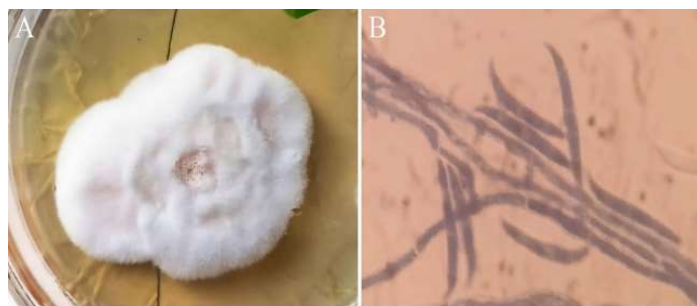


**Fig. (2).** (A) Colony of *F. oxysporum* displaying a white-pinkish hue on Potato Dextrose Agar (PDA) medium. (B) Microscopic view showing the characteristic sickle-shaped macroconidia of *F. oxysporum* with cross walls.

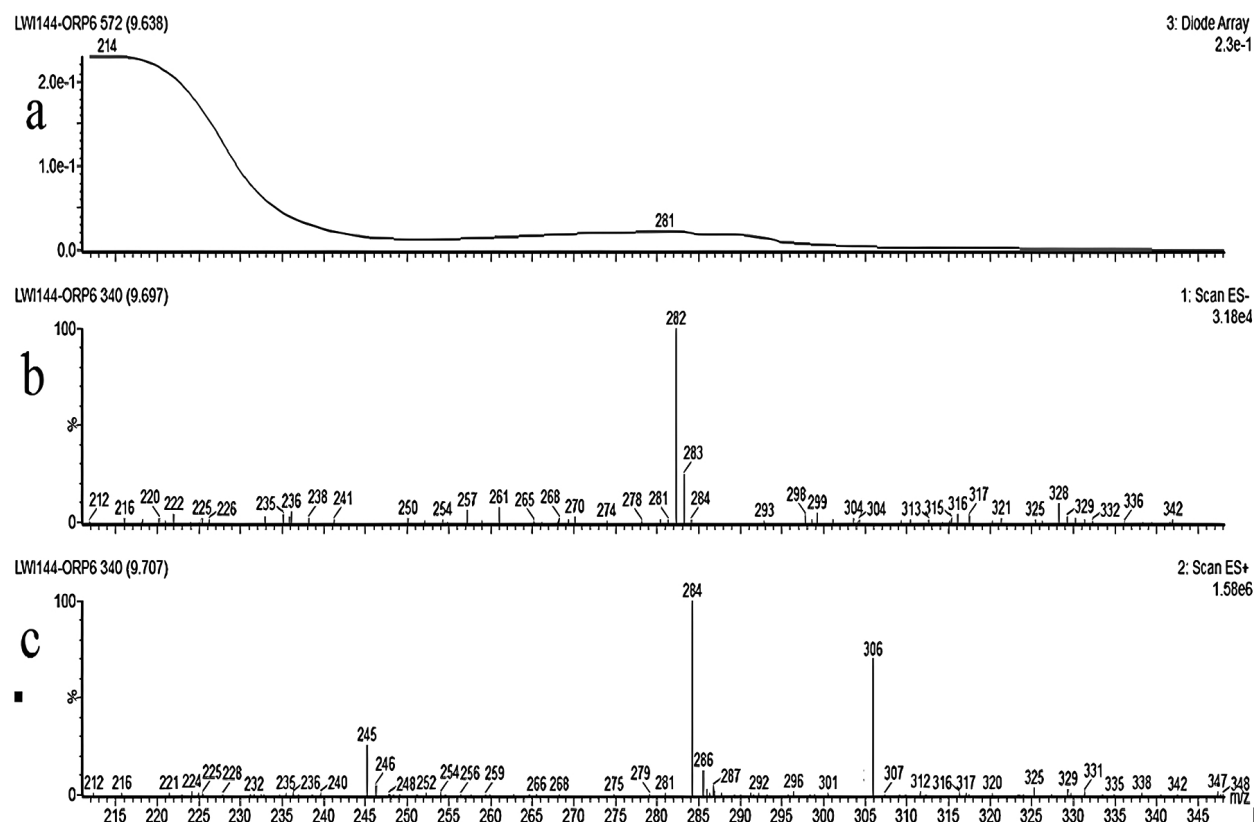


**Fig. (3).** Chromatogram of the pure compound acquired from the Waters LCMS system; Line a) displays the UV absorption spectrum of the compound (281  $\lambda_{\text{max}}$ ), indicating absorption at different wavelengths. Line b) represents the negative electrospray (ES-) profile of the compound, labeled as 282, while Line c) depicts the positive electrospray (ES+) profile, denoted as 284[M]<sup>+</sup>H and 306[M]<sup>+</sup>Na<sup>+</sup>.

### 3.3. Structure Elucidation/ Description of the Compound based on Data obtained from NMR

The structural determination of the compound was accomplished using a combination of  $^1\text{H}$ ,  $^{13}\text{C}$ ,  $^{15}\text{N}$ , and  $^{17}\text{O}$  NMR spectra, along with Heteronuclear Single Quantum Coherence (HSQC) spectroscopy. These spectra provided comprehensive insights into the different hydrogen, carbon, nitrogen, and oxygen environments within the molecule. The  $^1\text{H}$  NMR spectrum reveals multiple distinct peaks, each corresponding to different types of hydrogen environments within the molecule. The peak at  $\delta$  7.26 ppm indicates an NH proton, suggesting the presence of an amine group with strong hydrogen bonding. The peaks at  $\delta$  4.28 ppm and  $\delta$  4.11 ppm, corresponding to Atoms 2 (CH) and 10 (CH), suggest protons in relatively deshielded environments, likely adjacent to electronegative atoms or groups, such as oxygen or nitrogen. The peak at  $\delta$  6.44 ppm, corresponding to Atom 4 (CH), is indicative of a proton in an aromatic system or influenced by electron-withdrawing groups. Hydroxyl protons at  $\delta$  10.97 ppm and  $\delta$  4.19 ppm, corresponding to Atoms 13 (OH) and 15 (OH), respectively, indicate strong hydrogen bonding. The peaks at  $\delta$  2.05 ppm,  $\delta$  1.37 ppm, and  $\delta$  1.28 ppm, corresponding to Atoms 16 ( $\text{CH}_2$ ), 17 ( $\text{CH}_2$ ), and 18 ( $\text{CH}_2$ ), suggest these methylene groups are in an aliphatic chain. Terminal methyl groups at  $\delta$  0.97 ppm and  $\delta$  1.35 ppm, corresponding to Atoms 19 ( $\text{CH}_3$ ) and 20 ( $\text{CH}_3$ ), reflect their positions within the molecular framework and their relatively shielded environments.

The  $^{13}\text{C}$  NMR spectrum highlights various carbon environments within the molecule. The signal at  $\delta$  73.9 ppm for Atom 2 (CH) indicates a carbon adjacent to electronegative atoms, suggesting significant deshielding. The peaks at  $\delta$  145.1 ppm,  $\delta$  123.2 ppm, and  $\delta$  110.9 ppm, corresponding to Atoms 3 (C), 4 (CH), and 5 (C), respectively, suggest the presence of aromatic or olefinic carbons. The signals at  $\delta$  162.9 ppm and  $\delta$  159.7 ppm, corresponding to Atoms 6 (C) and 7 (C), indicate highly deshielded carbon environments, likely carbonyl groups, or similar functionalities. The peak at  $\delta$  66.1 ppm for Atom 10 (CH) suggests an aliphatic carbon adjacent to an electronegative atom. The methyl carbon signal at  $\delta$  23.7 ppm for Atom 11 ( $\text{CH}_3$ ) is typical for aliphatic methyl carbons. The resonance at  $\delta$  155.6 ppm for Atom 12 (C) suggests a carbonyl carbon. The signals at  $\delta$  33.8 ppm,  $\delta$  29.2 ppm, and  $\delta$  22.8 ppm for Atoms 16 ( $\text{CH}_2$ ), 17 ( $\text{CH}_2$ ), and 18 ( $\text{CH}_2$ ) confirm their aliphatic nature. The terminal methyl carbon signals at  $\delta$  14.0 ppm and  $\delta$  20.8 ppm for Atoms 19 ( $\text{CH}_3$ ) and 20 ( $\text{CH}_3$ ) indicate typical aliphatic environments.

The nitrogen  $^{15}\text{N}$  NMR spectrum provides additional insights into the oxygen environments within the compound. The peaks at  $\delta$  167.1 ppm,  $\delta$  306.0 ppm,  $\delta$  403.0 ppm,  $\delta$  248.1 ppm and  $\delta$  32.3 ppm, corresponding to Atoms 1 (O), 9 (O), 13 (OH), 14 (O), and 15 (OH), respectively, suggest the presence of various oxygen functionalities, such as hydroxyl and carbonyl groups, with the diverse chemical shifts reflecting their varied environments. The  $^{17}\text{O}$  NMR spectrum shows a significant peak at  $\delta$  -248.4 ppm for the

NH group at Atom 8, indicating a deshielded nitrogen environment, likely due to hydrogen bonding or an adjacent electronegative group. This chemical shift is consistent with nitrogen in amides or amines attached to carbonyl groups or within aromatic systems.

The HSQC spectrum provides correlations between proton and carbon atoms, confirming the assignments made from the proton and carbon NMR spectra by showing direct correlations between specific carbons and their attached hydrogens. For example, peaks in the aromatic region correlate aromatic protons with aromatic carbons, supporting the aromatic ring structure. Similarly, aliphatic protons and carbons show correlations that validate the presence of methylene and methyl groups. The spectrum highlights the detailed structure, showing which protons are bonded to which carbons, confirming the molecular framework suggested by the individual NMR spectra.

In conclusion, the integrated analysis of the  $^1\text{H}$ ,  $^{13}\text{C}$ ,  $^{15}\text{N}$ , and  $^{17}\text{O}$  NMR spectra, supported by HSQC correlations, reveals a complex organic molecule with the following features: an aromatic ring, aldehyde or conjugated systems, aliphatic chains, electronegative groups, amide or amine groups, and carbonyl and hydroxyl functionalities. This comprehensive NMR analysis reveals a molecule with aromatic characteristics, multiple functional groups, and varied carbon, nitrogen, and oxygen environments. The compound likely has a rich and complex structure, fitting the profile of many natural products with diverse functionalities. By integrating the information gathered from both spectra, the fungal compound is identified as (6-butyl-3-(1-hydroxyethyl)-2-methyl-2H-pyran-5-carbonyl) carbamic acid, revealing a complex arrangement featuring a substituted pyran ring, aliphatic chain, hydroxyl groups, and aromatic constituents (Fig. 4).

### 3.4. Molecular Docking Studies

The three-dimensional structure of the (6-butyl-3-(1-hydroxyethyl)-2-methyl-2H-pyran-5-carbonyl) was retrieved from Pubchem and prepared using BIOVIA Discovery Studio Visualizer. After preparation, the structure was used for docking analysis using the sigma glutathione transferase enzyme as a receptor. The docking analysis predicted -5.3 binding energy representing the selected compound has significant binding affinity for the target receptor. The docking analysis unveils that the screened compound could inhibit the target protein and block *Aphis gossypii* pathogenesis. Further, the docked complex confirmation analysis revealed that the selected compound has different interactions like van der Waals force, conventional hydrogen bonding, and carbon-hydrogen bonding, which are observed as different amino acids, and their interaction is presented in the following Fig. (5).

### 3.5. Molecular Dynamics Simulations

The static binding intermolecular conformation of the receptor and compound in docking studies was revalidated by molecular dynamics simulation assay to explore the complex dynamics on a given simulation period. The intermolecular binding mode stability of the complex was determined by two structure analyses such as root mean square

deviation (RMSD) and root mean square fluctuation (RMSF), both of which were done considering carbon alpha atoms of the complex. The RMSD depicts structural changes over the simulation time and as shown in the figure, the complex revealed a very stable RMSD plot demonstrating no major structure deviations. The mean RMSD of the complex is 1.45 angstroms. Little RMSD jumps were noticed, which were observed due to flexible complex loops, and were found not

to disturb the complex structure dynamics (Fig. 6). The residue level deviations were interpreted using root mean square fluctuations (RMSF) as given in Figure. The mean RMSF of the receptor in the presence of the compound is 1.58 angstroms with few sudden jumps, which corresponds to the receptor loops due to small compound pocket movements (Fig. 7).

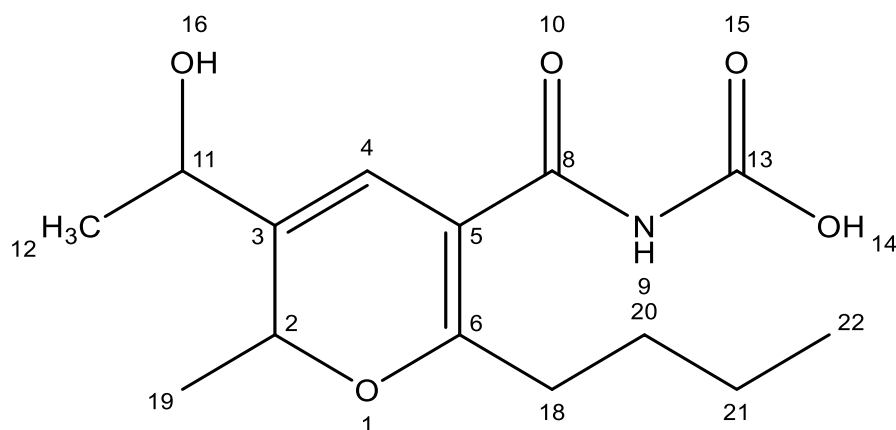


**Fig. (4).** Structure of the pure compound.

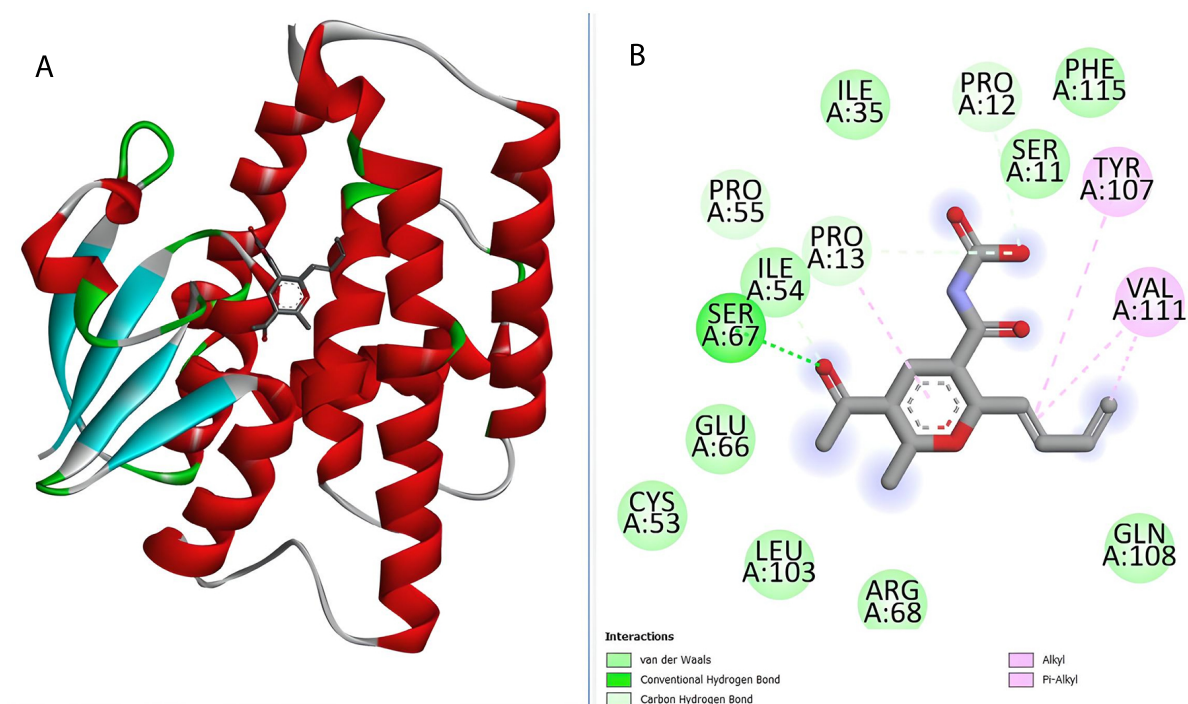


**Fig. (5).** (A) Represent the selected compound docked with targeted protein while (B) represents different binding interactions of compound (4-chloro-1-(methyl)- λ4-sulfaneyl)-1 λ5-phosphinine-3-carbonyl carbamic acid) and selected proteins (sigma glutathione transferase).

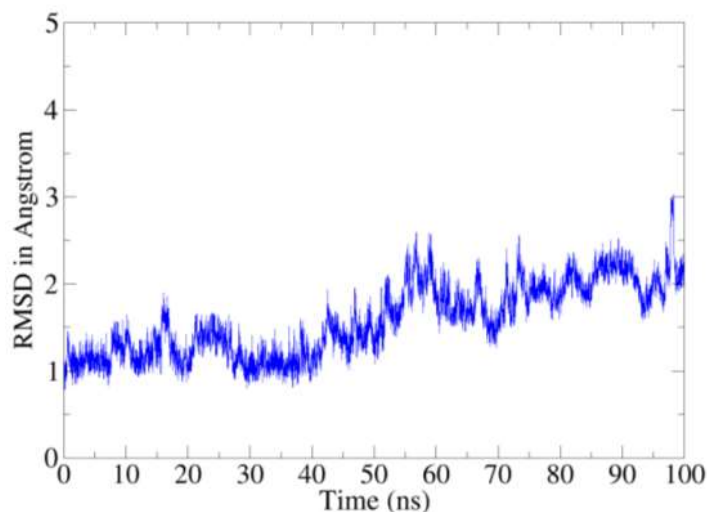


**Fig. (6).** RMSD based on carbon alpha atoms.

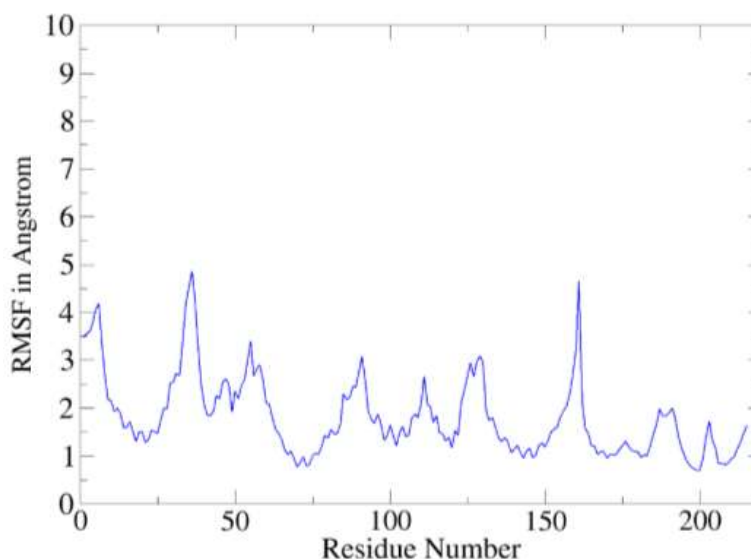


**Fig. (7).** RMSF analysis of the complex.

### 3.6. Binding Free Energies

The binding free energies for the compound in complex with the receptor enzyme were determined along the simulation trajectories. It was found that the intermolecular binding affinity was dominated by van der Waals forces, followed by electrostatic forces, while a negative contribution was seen from the solvation energy. The van der Waals, electrostatic, and solvation energy of the complex was -68.64 kcal/mol, -25.75 kcal/mol, and 10.58 kcal/mol, respectively. The total energy contribution of the complex was -83.81 kcal/mol, illustrating the formation of a highly stable complex. The Table shows details of the different energy contributions to the complex formation (Table 1).

**Table 1.** Binding energy contribution of the complex.

Parameter	Compound 283
Energy van der Waals	-68.64
Energy Electrostatic	-25.75
Total Gas Phase Energy	- 94.39
Total Solvation Energy	10.58
Net Energy	-83.81

### 3.7. In vitro Insecticidal Activity of the Compound

This experiment was conducted in triplicate, and the mean of the three trials was considered in the compilation



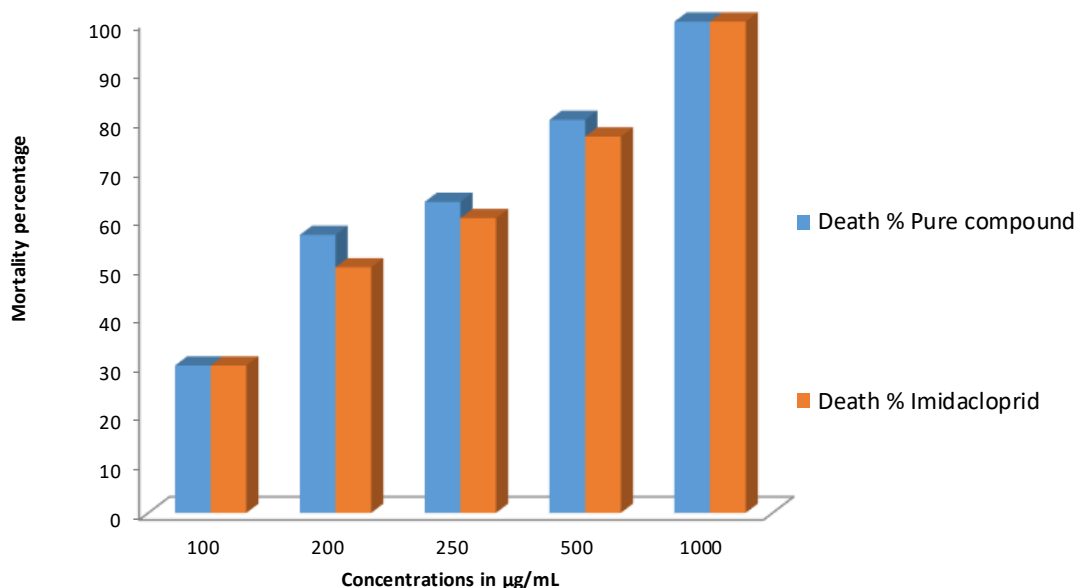


**Fig. (8).** Comparison of insecticidal activity of the purified fungal compound and the standard insecticide (Imidacloprid) against *Helicoverpa armigera* larvae at different concentrations. The Y-axis represents the mortality percentage of larvae, while the X-axis indicates the tested concentrations. The blue bars correspond to the mortality percentage induced by the pure compound, while the red bars represent the mortality percentage caused by Imidacloprid.

of results. The fungal compound, administered at concentrations of 100, 200, and 250  $\mu\text{g mL}^{-1}$ , exhibited mortality rates of 30%, 56.6%, and 63.3%, respectively. Specifically, at the 100  $\mu\text{g mL}^{-1}$  concentration, it resulted in the death of 3 larvae in each Petri plate. At the 200  $\mu\text{g mL}^{-1}$  concentration, 6, 6, and 5 larvae succumbed in the corresponding Petri plates, while at the 250  $\mu\text{g mL}^{-1}$  concentration, 6, 6, and 7 larvae were killed. In comparison, the standard drug, imidacloprid, demonstrated mortality rates of 30%, 50%, and 60% at the respective concentrations. At a concentration of 500  $\mu\text{g mL}^{-1}$ , the fungal compound inhibited the growth of 8 larvae in each test plate, resulting in an 80% mortality rate. Meanwhile, the standard at this concentration caused the death of 8 larvae in two Petri plates and 7 larvae in the third, resulting in a mortality rate of 76.6%. At the highest applied concentration (1000  $\mu\text{g mL}^{-1}$ ), both the fungal compound and the standard exhibited 100% mortality by inhibiting the growth of every larva in all Petri plates. The results of *in vitro* insecticidal activity are summarized in Fig. (8).

#### 4. DISCUSSION

Endophytic fungi are a prolific source of secondary metabolites with diverse applications, including antimicrobial, anticancer, and insecticidal properties. Commercial insecticides derived from fungal sources, such as Mcotrol [42], PFR-97 [43], and Met52 [44], highlight the significant potential of these natural products for effective pest management in agriculture. While the genera *Beauveria*, *Metarhizium*, and *Isaria* have been extensively studied for their insecticidal metabolites [45], *Fusarium* species, such as *Fusarium oxysporum* and *Fusarium solani* have also been

recognized for producing notable insecticidal compounds [46]. In the present study, we isolated *F. oxysporum* from the rhizosphere of ginger plants and purified four secondary metabolites. This study specifically concentrates on one of these purified compounds. The compound's structure was elucidated, and its potential as an insecticide was explored through comparative structural analysis, *in silico*, and *in vitro* studies. Our findings suggest that this compound could serve as an effective insecticide in agricultural settings, aligning with previous reports of *Fusarium* species producing insecticidal metabolites.

The structural features of the pure compound, 6-butyl-3-(1-hydroxyethyl)-2-methyl-2H-pyran-5-carbonyl carbamic acid, were compared to established insecticides, revealing several intriguing parallels. Insecticides from various chemical classes, including organophosphates, pyrethroids, neonicotinoids, and carbamates, function through diverse mechanisms targeting critical physiological processes in insects. The presence of a carbamate moiety in our compound suggests a mode of action similar to that of carbamate insecticides, which inhibit acetylcholinesterase, disrupting neural signaling in insects [47]. This structural resemblance implies potential neurotoxic effects akin to traditional carbamate insecticides. Furthermore, the substituted pyran ring in our compound evokes structural similarities with pyrethroid insecticides, known for their heterocyclic structures. Pyrethroids act by prolonging the opening of voltage-gated sodium channels in insect neurons, leading to hyperexcitation and paralysis [48]. The analogous structure suggests a comparable mechanism of action for our compound. Additionally, the aliphatic chain in the compound is reminiscent of the hydrophobic alkyl chains in synthetic pyrethroids, which enhance cuticular penetration and bin-

ding affinity to insect nerve membranes, increasing insecticidal potency [48].

The hydroxyl group within our compound bears a resemblance to functional groups found in neonicotinoid insecticides. Neonicotinoids act as agonists at nicotinic acetylcholine receptors in insects, disrupting neurotransmission and ultimately leading to paralysis and death [49]. This structural feature suggests potential interactions with similar target sites, implying a comparable mode of action. Based on the structural features of the purified compound, we hypothesized that the compound under study possesses inherent insecticidal properties. This hypothesis was experimentally validated through *in silico* and *in vitro* analyses, comparing the compound's efficacy with a standard insecticide, Imidacloprid.

The compound's *in vitro* insecticidal potential was evaluated against *H. armigera*. At the highest applied concentration (1000  $\mu\text{g mL}^{-1}$ ), both the fungal compound and Imidacloprid exhibited 100% mortality. However, at lower concentrations, the fungal compound demonstrated superior efficacy. Specifically, at concentrations of 100, 200, and 250  $\mu\text{g mL}^{-1}$ , the fungal compound achieved mortality rates of 30%, 56.6%, and 63.3%, respectively, compared to Imidacloprid's 30%, 50%, and 60%. At a concentration of 500  $\mu\text{g mL}^{-1}$ , the fungal compound resulted in an 80% mortality rate, compared to 76.6% for Imidacloprid. These results indicate that the fungal compound possesses significant insecticidal activity, even at lower concentrations. This feature is ecologically significant, as it allows for the use of lower concentrations of the insecticide to effectively control insect populations in agricultural settings. This approach potentially reduces environmental impact and the risk of developing resistance.

Our findings highlight the potential of the compound under study isolated from *F. oxysporum* as an effective insecticide. The superior efficacy at lower concentrations suggests it could be a valuable addition to integrated pest management strategies. However, further investigations into its precise mode of action, environmental impact, and field efficacy are necessary to fully understand its potential for sustainable agricultural pest management. Future studies should also explore the synthesis of analogs to optimize their insecticidal properties and assess their compatibility with other pest control methods. This preliminary investigation provides evidence for the insecticidal potential of the purified compound from *F. oxysporum*. The structural and experimental analyses offer insights into its mechanisms of action, supporting its candidacy as a potent insecticide. This work paves the way for developing new, ecologically friendly pest control solutions derived from fungal secondary metabolites.

## CONCLUSION

Based on the results obtained from the *in silico* and *in vitro* experiments, it is evident that the pure compound under study exhibits potent insecticidal potential. Molecular docking studies demonstrated a significant binding affinity for sigma glutathione transferase, with a binding energy of  $-5.3 \text{ kcal mol}^{-1}$ , indicating strong inhibitory potential. Molecular dynamics simulations confirmed the

stability of the compound-receptor complex, supported by consistent RMSD and RMSF values. The binding free energy analysis revealed that van der Waals forces predominantly drive the interaction, resulting in a net binding energy of  $-83.81 \text{ kcal mol}^{-1}$  suggesting a highly stable complex. Furthermore, the *in vitro* assay showed substantial larvicidal activity, with mortality rates reaching 100% at the highest concentration. From these collective findings, we conclude that this *F. oxysporum*-derived compound is a promising candidate for insecticide development and warrants further investigation for practical pest control applications.

## STUDY LIMITATION

This study serves as a preliminary investigation into the purification, characterization, structural elucidation, and potential applications of a bioactive compound derived from *Fusarium* species. Our primary objective was to explore its potential using *in silico* and *in vitro* analyses. However, certain limitations should be acknowledged.

The compound was isolated in a limited quantity, restricting us to conducting only a single *in vitro* bioassay. Due to this constraint, further biological evaluations, including comprehensive toxicity profiling and field trials, could not be performed at this stage. The small yield also limited detailed investigations into the compound's mechanism of action, metabolic stability, and selectivity, particularly regarding its potential effects on non-target organisms, including humans. Additionally, field trials, which are essential for assessing the compound's real-world insecticidal efficacy, could not be conducted. Despite these limitations, this study establishes a foundation for future research, emphasizing the need for chemical synthesis of the compound in larger quantities to enable further toxicity assessments, field applications, and environmental impact studies.

## PROSPECTS

This study lays the groundwork for further research into the bioactive potential of the purified *Fusarium*-derived compound, particularly as a promising eco-friendly insecticide. Future work will focus on chemical synthesis to produce the compound in sufficient quantities for comprehensive biological evaluations, including detailed toxicity profiling, selectivity assessments, and environmental safety studies. Additionally, field trials will be conducted to evaluate its real-world efficacy in pest management. Further investigations will explore its broader bioactive properties, such as antimicrobial, antifungal, or plant-growth-promoting activities, which could expand its potential applications in agriculture and biotechnology.

## AUTHORS' CONTRIBUTIONS

The authors confirm their contribution to the paper as follows: S.K.: Study conception and design; M.S.: Data collection; A.M.A.: Validation; S.A., D.Q.W., N.A.A.: Draft manuscript. All authors reviewed the results and approved the final version of the manuscript.

## LIST OF ABBREVIATIONS

PDA = Potato Dextrose Agar

CDA = Czapec Dox Agar  
 SDA = Saboraud Dextrose Agar  
 HCl = Hydrochloric acid  
 LCMS = Liquid Chromatography-mass Spectrometry  
 RMSD = Root Mean Square Deviation

## ETHICS APPROVAL AND CONSENT TO PARTICIPATE

Not applicable.

## HUMAN AND ANIMAL RIGHTS

Not Applicable.

## CONSENT FOR PUBLICATION

Not applicable.

## AVAILABILITY OF DATA AND MATERIALS

All data generated or analyzed during this study are included in this published article.

## FUNDING

King Saud University, Riyadh, Saudi Arabia, has funded the study under the project number (RSPD2025R1035).

## CONFLICT OF INTEREST

The authors declare no conflict of interest, financial or otherwise.

## ACKNOWLEDGEMENTS

The authors are thankful to the Researchers Supporting Project number (RSPD2025R1035), King Saud University, Riyadh, Saudi Arabia.

## REFERENCES

- [1] Sarwar S. Advancing sustainable agriculture: A comprehensive analysis of integrated pest management strategies in global rice production. *Int J Agric Sustain Dev* 2024; 6(1): 1-14.
- [2] Zhou W, Arcot Y, Medina RF, Bernal J, Cisneros-Zevallos L, Akbulut MES. Integrated pest management: An update on the sustainability approach to crop protection. *ACS Omega* 2024; 9(40): 41130-47. <http://dx.doi.org/10.1021/acsomega.4c06628> PMID: 39398119
- [3] Parven A, Meftaul IM, Venkateswarlu K. Herbicides in modern sustainable agriculture: Environmental fate, ecological implications, and human health concerns. *Int J Environ Sci Technol* 2025; 22: 1181-202. <http://dx.doi.org/10.1007/s13762-024-05818-y>
- [4] Ambaye TG, Hassani A, Vaccari M, *et al.* Emerging technologies for the removal of pesticides from contaminated soils and their reuse in agriculture. *Chemosphere* 2024; 362: 142433. <http://dx.doi.org/10.1016/j.chemosphere.2024.142433> PMID: 38815812
- [5] Duarte-Casar R. Synergies between green chemistry principles and the sustainable development goals (SDGs) in developing eco-friendly pesticides. *The Interplay of Pesticides and Climate Change: Environmental Dynamics and Challenges*. Cham: Springer 2025. [http://dx.doi.org/10.1007/978-3-031-81669-7\\_11](http://dx.doi.org/10.1007/978-3-031-81669-7_11)
- [6] Attri S. Seeds of sustainability: Promoting food security through eco-friendly agriculture. *Sustainable Synergy: Harnessing Ecosystems for Climate Resilience Climate Change Management*. Cham: Springer 2025; pp. 83-97. [http://dx.doi.org/10.1007/978-3-031-77957-2\\_6](http://dx.doi.org/10.1007/978-3-031-77957-2_6)
- [7] Wadhwa K, Kapoor N, Kaur H, *et al.* A comprehensive review of the diversity of fungal secondary metabolites and their emerging applications in healthcare and environment. *Mycobiology* 2024; 52(6): 335-87. <http://dx.doi.org/10.1080/12298093.2024.2416736> PMID: 39845176
- [8] Bendejacq-Seychelles A, Gibot-Leclerc S, Guillemin JP, Mouille G, Steinberg C. Phytotoxic fungal secondary metabolites as herbicides. *Pest Manag Sci* 2024; 80(1): 92-102. <http://dx.doi.org/10.1002/ps.7813> PMID: 37794581
- [9] Abd-Elsalam KA. Hidden biocontrol agents: The world of insect-pathogenic fungi. *Fungal Endophytes Volume I: Biodiversity and Bioactive Materials*. Singapore: Springer 2025; pp. 301-39. [http://dx.doi.org/10.1007/978-981-97-7312-1\\_11](http://dx.doi.org/10.1007/978-981-97-7312-1_11)
- [10] Saha N, Sharma A, Bora P. Expanding the functional landscape of microbial entomopathogens in agriculture beyond pest management. *Folia Microbiol* 2025; 1-15. <http://dx.doi.org/10.1007/s12223-025-01251-x> PMID: 40042570
- [11] Singh VK, Kumar A. Secondary metabolites from endophytic fungi: Production, methods of analysis, and diverse pharmaceutical potential. *Symbiosis* 2023; 90(2): 111-25. <http://dx.doi.org/10.1007/s13199-023-00925-9> PMID: 37360552
- [12] Kim JC, Hwang IM, Kim HM, *et al.* Rapid analysis of insecticidal metabolites from the entomopathogenic fungus *Beauveria bassiana* 331R using UPLC-Q-Orbitrap MS. *Mycotoxin Res* 2024; 40(1): 123-32. <http://dx.doi.org/10.1007/s12550-023-00509-y> PMID: 37968430
- [13] Vivekanandhan P, Swathy K, Bedini S, Shivakumar MS. Bioprospecting of *Metarhizium anisopliae* derived crude extract: A ecofriendly insecticide against insect pest. *Int J Trop Insect Sci* 2023; 43(2): 429-40. <http://dx.doi.org/10.1007/s42690-022-00935-y>
- [14] Feiqian D, Jiachan Z, Wenjing C, Luyao L, Meng L, Changtao W. *Paecilomyces cicadae* : A systematic overview of the biological activities and potential mechanisms of its active metabolites. *Food Agric Immunol* 2023; 34(1): 2243059. <http://dx.doi.org/10.1080/09540105.2023.2243059>
- [15] Wijayawardene N, Boonyuen N, Ranaweera C, *et al.* OMICS and other advanced technologies in mycological applications. *J Fungi* 2023; 9(6): 688. <http://dx.doi.org/10.3390/jof9060688> PMID: 37367624
- [16] Gayathiri E, Prakash P, Kumaravel P, *et al.* Computational approaches for modeling and structural design of biological systems: A comprehensive review. *Prog Biophys Mol Biol* 2023; 185: 17-32. <http://dx.doi.org/10.1016/j.pbiomolbio.2023.08.002> PMID: 37821048
- [17] Bogari HA, Elhady SS, Darwish KM, *et al.* Molecular and biological investigation of isolated marine fungal metabolites as anticancer agents: A multi-target approach. *Metabolites* 2023; 13(2): 162. <http://dx.doi.org/10.3390/metabo13020162> PMID: 36837781
- [18] Shafiq N, Shakoob B, Yaqoob N, *et al.* A virtual insight into mushroom secondary metabolites: 3D-QSAR, docking, pharmacophore-based analysis and molecular modeling to analyze their anti-breast cancer potential. *J Biomol Struct Dyn* 2024; 1-22. <http://dx.doi.org/10.1080/07391102.2024.2304137> PMID: 38299565
- [19] Siddiqui JA, Fan R, Naz H, *et al.* Insights into insecticide-resistance mechanisms in invasive species: Challenges and control strategies. *Front Physiol* 2023; 13: 1112278. <http://dx.doi.org/10.3389/fphys.2022.1112278> PMID: 36699674
- [20] Wilberts L. Use of endophytic entomopathogenic fungi to improve biological control of pest insects. 2023.
- [21] Tiwari P, Bae H. Endophytic fungi: Key insights, emerging prospects, and challenges in natural product drug discovery. *Microorganisms* 2022; 10(2): 360. <http://dx.doi.org/10.3390/microorganisms10020360> PMID: 35815812

- 35208814
- [22] Massoud MS, Ahmed Khalil DM. Fungi associated with ornamental plants in some Nurseries in Al-Qurayyat, Jouf region, Saudi Arabia. *Iran J Microbiol* 2023; 15(1): 174-80.  
<http://dx.doi.org/10.18502/ijm.v15i1.11934> PMID: 37069907
  - [23] Aoki T. Comparative taxonomic studies on Fusarium, especially those species harmful to plants. *J Gen Plant Pathol* 2022; 88(6): 408-12.  
<http://dx.doi.org/10.1007/s10327-022-01085-2>
  - [24] Leslie JF, Summerell BA. The Fusarium laboratory manual. John Wiley & Sons 2008.
  - [25] Westblade LF. Larone's Medically Important Fungi: A Guide to Identification. John Wiley & Sons 2023.
  - [26] Frisvad JC. Media and growth conditions for induction of secondary metabolite production. *Methods Mol Biol* 2012; 944: 47-58.  
[http://dx.doi.org/10.1007/978-1-62703-122-6\\_3](http://dx.doi.org/10.1007/978-1-62703-122-6_3)
  - [27] Westphal KR, Heidelberg S, Zeuner EJ, et al. The effects of different potato dextrose agar media on secondary metabolite production in Fusarium. *Int J Food Microbiol* 2021; 347: 109171.  
<http://dx.doi.org/10.1016/j.ijfoodmicro.2021.109171> PMID: 33872940
  - [28] Mohammed AE, Sonbol H, Alwakeel SS, et al. Investigation of biological activity of soil fungal extracts and LC/MS-QTOF based metabolite profiling. *Sci Rep* 2021; 11(1): 4760.  
<http://dx.doi.org/10.1038/s41598-021-83556-8> PMID: 33637771
  - [29] Keshri PK, Rai N, Verma A, et al. Biological potential of bioactive metabolites derived from fungal endophytes associated with medicinal plants. *Mycol Prog* 2021; 20(5): 577-94.  
<http://dx.doi.org/10.1007/s11557-021-01695-8>
  - [30] Jakhar R, Dangi M, Khichi A, Chhillar AK. Relevance of molecular docking studies in drug designing. *Curr Bioinform* 2020; 15(4): 270-8.  
<http://dx.doi.org/10.2174/1574893615666191219094216>
  - [31] Udomsinprasert R, Pongjaroenkit S, Wongsantichon J, et al. Identification, characterization and structure of a new Delta class glutathione transferase isoenzyme. *Biochem J* 2005; 388(3): 763-71.  
<http://dx.doi.org/10.1042/BJ20042015> PMID: 15717864
  - [32] Pettersen EF, Goddard TD, Huang CC, et al. UCSF Chimera—A visualization system for exploratory research and analysis. *J Comput Chem* 2004; 25(13): 1605-12.  
<http://dx.doi.org/10.1002/jcc.20084> PMID: 15264254
  - [33] Dallakyan S, Olson AJ. Small-molecule library screening by docking with PyRx. *Methods Mol Biol* 2015; 1263: 243-50.  
[http://dx.doi.org/10.1007/978-1-4939-2269-7\\_19](http://dx.doi.org/10.1007/978-1-4939-2269-7_19)
  - [34] Studio D. Discovery studio. Accelrys 2008; 420: 1-9.
  - [35] Case DA. AMBER 22 reference manual. 2022. Available from: <https://ambermd.org/doc12/Amber22.pdf>
  - [36] Tian C, Kasavajhala K, Belfon KAA, et al. ff19SB: Amino-acid-specific protein backbone parameters trained against quantum mechanics energy surfaces in solution. *J Chem Theory Comput* 2020; 16(1): 528-52.  
<http://dx.doi.org/10.1021/acs.jctc.9b00591> PMID: 31714766
  - [37] Vassetti D, Pagliai M, Procacci P. Assessment of GAFF2 and OPLS-AA general force fields in combination with the water models TIP3P, SPCE, and OPC3 for the solvation free energy of druglike organic molecules. *J Chem Theory Comput* 2019; 15(3): 1983-95.  
<http://dx.doi.org/10.1021/acs.jctc.8b01039> PMID: 30694667
  - [38] Ahmad S, Raza S, Uddin R, Azam SS. Binding mode analysis, dynamic simulation and binding free energy calculations of the MurF ligase from *Acinetobacter baumannii*. *J Mol Graph Model* 2017; 77: 72-85.  
<http://dx.doi.org/10.1016/j.jmgm.2017.07.024> PMID: 28843462
  - [39] Paquet E, Viktor HL. Molecular dynamics, monte carlo simulations, and langevin dynamics: A computational review. *BioMed Res Int* 2015; 2015(1): 1-18.  
<http://dx.doi.org/10.1155/2015/183918> PMID: 25785262
  - [40] Roe DR, Cheatham TE III. PTRAJ and CPPTRAJ: Software for processing and analysis of molecular dynamics trajectory data. *J Chem Theory Comput* 2013; 9(7): 3084-95.  
<http://dx.doi.org/10.1021/ct400341p> PMID: 26583988
  - [41] Miller BR III, McGee TD Jr, Swails JM, Homeyer N, Gohlke H, Roitberg AE. MMPBSA.py: An efficient program for end-state free energy calculations. *J Chem Theory Comput* 2012; 8(9): 3314-21.  
<http://dx.doi.org/10.1021/ct300418h> PMID: 26605738
  - [42] Patra S. Microbes as Biocontrol. Microbial Approaches for Sustainable Green Technologies. CRC Press 2024; p. 196.
  - [43] Bohatá A, Folorunso EA, Lencová J, Osborne LS, Mraz J. Control of sweet potato whitefly (*Bemisia tabaci*) using entomopathogenic fungi under optimal and suboptimal relative humidity conditions. *Pest Manag Sci* 2024; 80(3): 1065-75.  
<http://dx.doi.org/10.1002/ps.7837> PMID: 37842745
  - [44] Wood MJ, Kortsinoglou AM, Bull JC, et al. Evaluation of *Metarhizium brunneum*-and *Metarhizium*-derived VOCs as dual-active biostimulants and pest repellents in a wireworm-infested potato field. *J Fungi* 2023; 9(6): 599.  
<http://dx.doi.org/10.3390/jof9060599> PMID: 37367536
  - [45] Shahbaz M, Palaniveloo K, Tan YS, et al. Entomopathogenic fungi in crops protection with an emphasis on bioactive metabolites and biological activities. *World J Microbiol Biotechnol* 2024; 40(7): 217.  
<http://dx.doi.org/10.1007/s11274-024-04022-x> PMID: 38806748
  - [46] Santos ACS, Diniz AG, Tiago PV, Oliveira NT. Entomopathogenic Fusarium species: A review of their potential for the biological control of insects, implications and prospects. *Fungal Biol Rev* 2020; 34(1): 41-57.  
<http://dx.doi.org/10.1016/j.fbr.2019.12.002>
  - [47] Eldefrawi ME, Eldefrawi AT. Nervous-system-based insecticides. Safer Insecticides. CRC Press 2020; pp. 155-207.
  - [48] de Brum Vieira P. The effects of pyrethroids on the mitochondria. Mitochondrial Intoxication. Elsevier 2023; pp. 683-705.  
<http://dx.doi.org/10.1016/B978-0-323-88462-4.00019-5>
  - [49] Zuščíková L, Bažány D, Greifová H, et al. Screening of toxic effects of neonicotinoid insecticides with a focus on acetamiprid: A review. *Toxics* 2023; 11(7): 598.  
<http://dx.doi.org/10.3390/toxics11070598> PMID: 37505564